

# $\alpha$ v $\beta$ 3 and $\alpha$ 5 $\beta$ 1 integrin recycling pathways dictate downstream Rho kinase signaling to regulate persistent cell migration

Dominic P. White, Patrick T. Caswell, and Jim C. Norman

Integrin Cell Biology Laboratory, Beatson Institute for Cancer Research, Bearsden, Glasgow G61 1BD, Scotland, UK

**A**ccumulating evidence suggests that integrin recycling regulates cell migration. However, the lack of reagents to selectively target the trafficking of individual heterodimers, as opposed to endocytic transport as a whole, has made it difficult to define the contribution made by particular recycling pathways to directional cell movement. We show that autophosphorylation of protein kinase D1 (PKD1) at Ser<sup>916</sup> is necessary for its association with  $\alpha$ v $\beta$ 3 integrin. Expression of PKD1<sup>916A</sup> or the use of

mutants of  $\beta$ 3 that do not bind to PKD1 selectively inhibits short-loop, Rab4-dependent recycling of  $\alpha$ v $\beta$ 3, and this suppresses the persistence of fibroblast migration. However, we report that short-loop recycling does not directly contribute to fibroblast migration by moving  $\alpha$ v $\beta$ 3 to the cell front, but by antagonizing  $\alpha$ 5 $\beta$ 1 recycling, which, in turn, influences the cell's decision to migrate with persistence or to move randomly.

## Introduction

A detailed molecular understanding of the mechanisms by which cells migrate is important not only to our view of normal physiological processes, such as embryonic development and wound repair, but also to our ability to intervene in the progression of inflammatory disease and cancer. The integrin family of heterodimeric matrix receptors plays a central role in normal and pathophysiological modes of cell migration by acting not only to physically couple cells to the ECM but also to function as signaling molecules that transmit information across the plasma membrane (Hynes, 2002). Of the numerous intracellular signaling events that are triggered by integrin engagement, perhaps the most pertinent to cell migration is their capacity to influence cytoskeletal dynamics via the activation of Rho subfamily GTPases (Cox et al., 2001; Arthur et al., 2002). Indeed, cells can use different migrational modes to move with varying degrees of speed and directionality depending on the nature of Rho GTPase signaling downstream of integrins. For instance, metastasizing tumor cells often move randomly and rapidly undergo amoeboid shape changes, and this depends on the ability of  $\beta$ 1 integrins to activate Rho kinase (ROCK) via the small GTPase, RhoA (Vial et al., 2003). Alternatively, during

processes such as wound healing, fibroblasts migrate directionally and with high persistence (i.e., the tendency to continue traveling in the same direction without turning), and this can be determined by the degree of Rac signaling downstream of  $\alpha$ 5 $\beta$ 1 integrin (Pankov et al., 2005).

To an extent, patterns of migratory behavior are dictated by characteristics that are intrinsic to particular cell types. However, both normal cells and those derived from tumors can switch between different modes of migration, and signaling pathways activated downstream of integrins can contribute to this. For instance, epithelial cells expressing  $\alpha$ v $\beta$ 3 integrin migrate persistently, but the same cells migrate randomly upon expression of the  $\alpha$ 5 $\beta$ 1 heterodimer (Danan et al., 2005). This is a consequence of the ability of  $\alpha$ 5 $\beta$ 1 to activate ROCK, which in turn phosphorylates and inhibits the actin-severing protein cofilin.

Several integrins engage in endo-exocytic cycling, and many of the Rab GTPases and kinases that control their return to the plasma membrane are now becoming clear (Caswell and Norman, 2006; Jones et al., 2006).  $\alpha$ 5 $\beta$ 1 integrin recycles to the plasma membrane from a perinuclear recycling compartment via a “long-loop” pathway requiring Rab11 and activity of the PKB/GSK-3 $\beta$  axis (Roberts et al., 2004). Conversely,  $\alpha$ v $\beta$ 3 integrin travels more rapidly back to the cell surface via a “short loop” that is controlled by Rab4 and requires association of protein kinase D1 (PKD1) with the integrin (Woods et al., 2004). Receptors for growth factors and chemokines are also endocytosed and then recycled back to the cell surface, and it is now

Correspondence to Jim C. Norman: j.norman@beatson.gla.ac.uk

Abbreviations used in this paper: MTOC, microtubule organizing center; PKD1, protein kinase D1; PMA, phorbol myristate acetate; ROCK, Rho kinase; shRNA, short hairpin RNA; ts, temperature-sensitive; VSVG, vesicular stomatitis virus G protein.

The online version of this article contains supplemental material.

clear that this process influences the way they signal (Miaczynska et al., 2004). Indeed, many receptors remain competent to signal in endosomal compartments, and recycling pathways can resensitize receptors to prolong signaling outputs, as is the case for CXCRs (Fan et al., 2004) and the  $\beta$ -adrenergic receptor (Odley et al., 2004). Furthermore, a recent study has suggested that recycling acts to constantly retarget internalized receptor tyrosine kinases to the leading edge, thus keeping downstream signaling localized during the directional migration of *Drosophila melanogaster* border cells (Jekely et al., 2005).

It has been proposed that receptor recycling pathways act to transport integrins forward during cell migration (Bretscher, 1996). Indeed, the localization of  $\alpha\text{v}\beta\text{3}$  integrin to focal complexes at the front of migrating cells is dependent on the short-loop pathway (Woods et al., 2004; Jones et al., 2006), but how this contributes to migration is not yet clear. It is possible that anterograde vesicular transport could contribute directly to persistent migration by constantly retargeting integrins to the leading edge, thus reinforcing the cell's polarity axis. Alternatively, trafficking may influence migrational modes by altering integrin signaling. The precise mechanistic link between integrins and Rho signaling is as yet undefined, and endosomal recycling pathways provide an interesting means of reconciling the respective localizations of integrins and their Rho signaling counterparts.

To resolve these issues, we have developed a strategy to target short-loop  $\alpha\text{v}\beta\text{3}$  recycling and have precisely determined its contribution to the speed and persistence of cell migration. Indeed, we find that short-loop recycling has a profound effect on the persistence of migration. This is not, however, because of its ability to transport  $\alpha\text{v}\beta\text{3}$  forward during cell migration but, rather, because it can antagonize  $\alpha\text{5}\beta\text{1}$  recycling and the signaling of this integrin to cofilin. Thus, we have revealed that vesicular transport makes a major contribution to cell migration via its capacity to dictate the nature of downstream integrin signaling, which in turn influences the migrational mode of fibroblasts.

## Results

### Phosphorylation at Ser<sup>916</sup> is necessary for PKD1- $\alpha\text{v}\beta\text{3}$ integrin association

We previously found that PKD1 can associate specifically with  $\alpha\text{v}\beta\text{3}$  integrin via a motif contained within the C-terminal 14 amino acids of the  $\beta\text{3}$  cytodomain (Woods et al., 2004). This association recruits PKD1 to  $\alpha\text{v}\beta\text{3}$  at endosomes and drives the rapid return of the heterodimer to the plasma membrane in response to growth factor treatment. To further characterize this integrin-kinase interaction, we expressed His-tagged PKD1 in Cos-1 cells and purified the kinase to near homogeneity by Ni-affinity chromatography (Fig. 1 A). To ensure a preparation of maximally active kinase, Cos-1 cells were treated with phorbol myristate acetate (PMA) for 30 min before lysis in the presence of phosphatase inhibitors. Purified PKD1 bound directly and with high affinity ( $K_d$  [apparent] in the low nanomolar range) to GST- $\beta\text{3}$  integrin cytodomain (Fig. 1 B). There was no detectable association between purified active PKD1 and the cytoplasmic sequences of the  $\alpha\text{v}$ ,  $\alpha\text{5}$ , or  $\beta\text{1}$  integrin subunits, indicating that the interaction was specific for  $\beta\text{3}$  integrin.

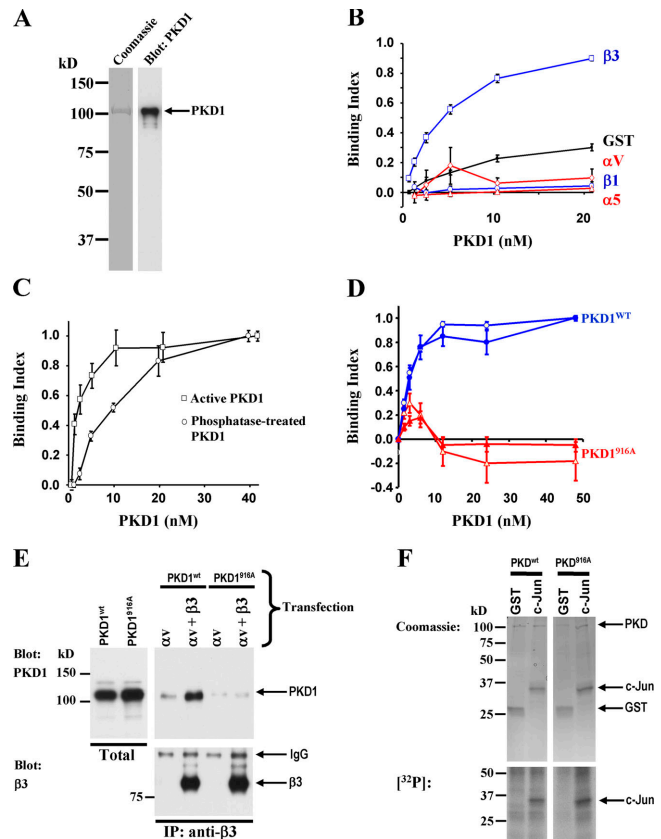


**Figure 1. Phosphorylation of Ser<sup>916</sup> is required for PKD1 to associate with  $\alpha\text{v}\beta\text{3}$  integrin.** (A) Cos-1 cells expressing His-PKD1 were treated with 1  $\mu\text{M}$  PMA for 15 min to activate the kinase and then lysed in a buffer containing phosphatase inhibitors. His-PKD1 was purified from the lysate by Ni-affinity chromatography and analyzed by SDS-PAGE followed by staining with colloidal Coomassie (left) or by Western blotting with anti-PKD1 (right). (B) GST fusion proteins of the indicated integrin cytodomains were immobilized on the surface of microtitre wells and incubated with serial dilutions of purified His-PKD1. Bound PKD1 was detected by ELISA using antibodies recognizing PKD1, followed by chromogenic detection with  $\alpha$ -phenylenediamine (Roberts et al., 2001). Values are mean  $\pm$  SEM ( $n > 5$ ). (C) Purified His-PKD1 was incubated in the presence or absence of alkaline phosphatase and then added to microtitre wells that had been previously coated with GST- $\beta\text{3}$  cytodomain. Bound PKD1 was detected by ELISA as for B. Values are mean  $\pm$  SEM ( $n = 4$ ). (D) His-PKD1<sup>WT</sup> and His-PKD1<sup>S916A</sup> were expressed in Cos-1 cells and purified as for A. Binding to GST- $\beta\text{3}$  was determined as for B. Two GST- $\beta\text{3}$  cytodomain constructs were used for these experiments; open and closed symbols indicate binding to GST- $\beta\text{3}^{727-762}$  and GST- $\beta\text{3}^{749-762}$ , respectively. Values are mean  $\pm$  SEM ( $n > 5$ ). (E) Mouse NIH3T3 fibroblasts were transfected with PKD1<sup>WT</sup> or PKD1<sup>S916A</sup> in conjunction with human  $\alpha\text{v}\beta\text{3}$  integrin or the  $\alpha\text{v}$  chain alone. Cells were treated with a combination of PDGF and primaquine for 12 min followed by lysis in a buffer containing 1% octyl  $\beta$ -thioglycolpyranoside. Lysates were incubated with magnetic beads coupled to an antibody recognizing human  $\beta\text{3}$  integrin for 2 h at 4°C. Immobilized material was analyzed by Western blotting for PKD1 (top) and  $\beta\text{3}$  integrin (bottom). (F) Purified His-PKD1<sup>WT</sup> or His-PKD1<sup>S916A</sup> was incubated with GST or GST-c-Jun in the presence of [<sup>32</sup>P]ATP. Phosphorylated proteins were visualized by SDS-PAGE followed by autoradiography (bottom), and protein loading was confirmed by staining with Coomassie blue.

After activation with growth factors, cellular PKD1 is phosphorylated at several residues (Vertommen et al., 2000). As we have previously shown that treatment with a growth factor such as PDGF is necessary for coimmunoprecipitation of  $\alpha\text{v}\beta\text{3}$  and PKD1 (Woods et al., 2004), we sought to determine whether phosphorylation was necessary for integrin binding.

Indeed, treatment of PKD1 with alkaline phosphatase (which led to ~80% dephosphorylation of the kinase [not depicted]) reduced the affinity of integrin–kinase association by approximately fivefold (Fig. 1 C). PKD1 is auto- (and possibly trans-) phosphorylated at Ser<sup>916</sup> in its C terminus (Matthews et al., 1999; Vertommen et al., 2000; Sanchez-Ruiloba et al., 2006), but no clear cellular role for this has been described. We therefore mutated Ser<sup>916</sup> of PKD1 to alanine and determined the ability of this mutant kinase to bind to  $\alpha\text{v}\beta\text{3}$  integrin. Indeed, purified PKD1<sup>916A</sup> had strikingly reduced ability to bind to GST fusion proteins of the  $\beta\text{3}$  integrin cytodomain (Fig. 1 D). Moreover, when expressed in fibroblasts, PKD1<sup>916A</sup> did not coimmunoprecipitate with  $\alpha\text{v}\beta\text{3}$  (Fig. 1 E), indicating that autophosphorylation of this residue is a prerequisite for integrin–kinase association. In agreement with a previous report (Vertommen et al., 2000), we found that mutation of Ser<sup>916</sup> had no influence on the PKD1 activity, as determined by the ability of purified PKD1<sup>916A</sup> to phosphorylate one of its best-characterized substrates, the N-terminal portion of c-Jun (Hurd et al., 2002; Fig. 1 F).

#### Expression of PKD1<sup>916A</sup> selectively opposes short-loop recycling of $\alpha\text{v}\beta\text{3}$

Suppression of cellular PKD1 levels by RNAi, expression of catalytically inactive PKD1s, and/or mutant  $\beta\text{3}$  subunits that cannot bind to PKD1 oppose short-loop recycling of  $\alpha\text{v}\beta\text{3}$  (Woods et al., 2004). However, these strategies will be likely to compromise other aspects of PKD1 and integrin signaling, such as the recruitment of c-Src to  $\alpha\text{v}\beta\text{3}$  (Arias-Salgado et al., 2003) and the role of PKD1 in Golgi transport (Liljedahl et al., 2001). With this in mind, we determined the influence of PKD1<sup>916A</sup> on integrin recycling via the short-loop pathway but also quantified other indices of integrin, PKD1, and endocytic function. Short-loop  $\alpha\text{v}\beta\text{3}$  recycling was driven by the addition of growth factors such as PDGF and lysophosphatidic acid and by the addition of 10% serum (all of which lead to PKD1 activation) to serum-starved cells (Fig. 2, A and B). However, after expression of PKD1<sup>916A</sup>, these agents were unable to drive the delivery of  $\alpha\text{v}\beta\text{3}$  to the plasma membrane, indicating that this PKD1 mutant acts in a dominant-negative fashion to oppose growth factor–driven short-loop integrin recycling (Fig. 2, A and B). Moreover, PKD1<sup>916A</sup> did not inhibit the return of integrins to the plasma membrane via the long loop (Fig. 2 C), the recycling of internalized [<sup>125</sup>I]Tfn (Fig. 2 D), or the endocytosis of integrins and the Tfn-R (not depicted), indicating that this mutant PKD1 selectively targets short-loop  $\alpha\text{v}\beta\text{3}$  recycling.

To gain information as to how PKD1<sup>916A</sup> exerts this dominant-negative effect on  $\alpha\text{v}\beta\text{3}$  recycling, we overexpressed His-tagged PKDs and measured activation of the endogenous kinase using a reporter antibody recognizing activating phosphorylations within the kinase domain of PKD1 (phospho-Ser<sup>744/8</sup>). Indeed, expression of His-PKD1 or His-PKD1<sup>916A</sup> strongly suppressed phosphorylation of the endogenous kinase at Ser<sup>744/8</sup> (Fig. S1, available at <http://www.jcb.org/cgi/content/full/jcb.200609004/DC1>), indicating that these overexpressed recombinant kinases can compete effectively with endogenous PKD1 for the upstream activating kinase (PKC $\epsilon$ ) that phosphorylates

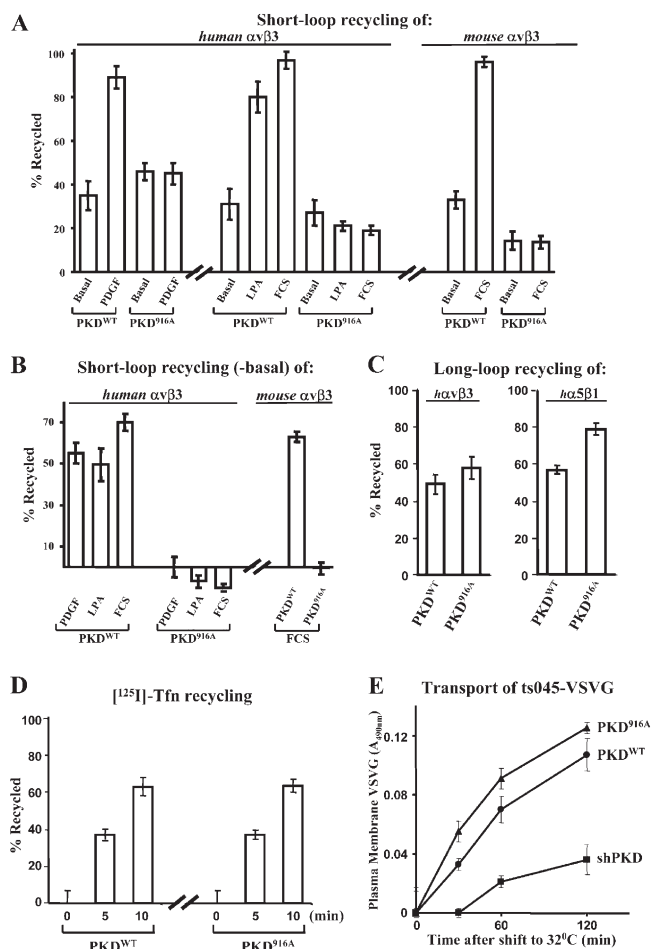


**Figure 2. PKD1<sup>916A</sup> opposes short-loop recycling of  $\alpha\text{v}\beta\text{3}$  integrin without inhibiting long-loop recycling or VSVG transport.** (A) NIH3T3 fibroblasts were transfected with  $\alpha\text{v}\beta\text{3}$  (human sequence) integrin in combination with PKD1<sup>WT</sup> or PKD1<sup>916A</sup> as indicated. Short-loop recycling in the presence or absence of 10 ng/ml PDGF-BB, 1 mg/ml lysophosphatidic acid (LPA), or 10% FCS was determined as described previously (Woods et al., 2004). To determine recycling of endogenous mouse  $\alpha\text{v}\beta\text{3}$ , NIH3T3 fibroblasts were transfected with PKD1<sup>WT</sup> or PKD1<sup>916A</sup> using the Nucleofector. Short-loop recycling of mouse  $\alpha\text{v}\beta\text{3}$  in the presence and absence of 10% FCS was determined as described by Roberts et al. (2001). (B) To evaluate the stimulus-dependent component of recycling, the data from A are presented after subtraction of the appropriate basal values. (C) Cells were transfected with  $\alpha\text{v}\beta\text{3}$  (left) or  $\alpha\text{5}\beta\text{1}$  (right) in combination with PKD1<sup>WT</sup> or PKD1<sup>916A</sup>. Long-loop recycling was determined as described previously (Roberts et al., 2001, 2004). (D) NIH3T3 fibroblasts were transfected with PKD1<sup>WT</sup> or PKD1<sup>916A</sup> using the Nucleofector. Cells were then incubated with [<sup>125</sup>I]transferrin for 1 h at 4°C to label the transferrin receptor at the cell surface. The tracer was allowed to internalize for 15 min at 22°C, and its return to the plasma membrane was determined as described previously (Roberts et al., 2004). (E) NIH3T3 fibroblasts were transfected with ts045 VSVG and placed at 40°C for 24 h. Cells were then incubated at 32°C for the indicated times and placed on ice. Surface proteins were labeled by incubation with NHS-Biotin (0.2 mg/ml) for 30 min at 4°C, and biotinylated VSVG was detected by capture ELISA using microtitre wells coated with a polyclonal antibody recognizing VSVG. Values are mean  $\pm$  SEM ( $n > 10$ ).

these residues, thus providing a mechanistic rationale for the dominant-negative influence of PKD1<sup>916A</sup> on integrin  $\alpha\text{v}\beta\text{3}$  recycling and function.

To assess TGN to plasma membrane transport, we used vesicular stomatitis virus G protein (VSVG) from the



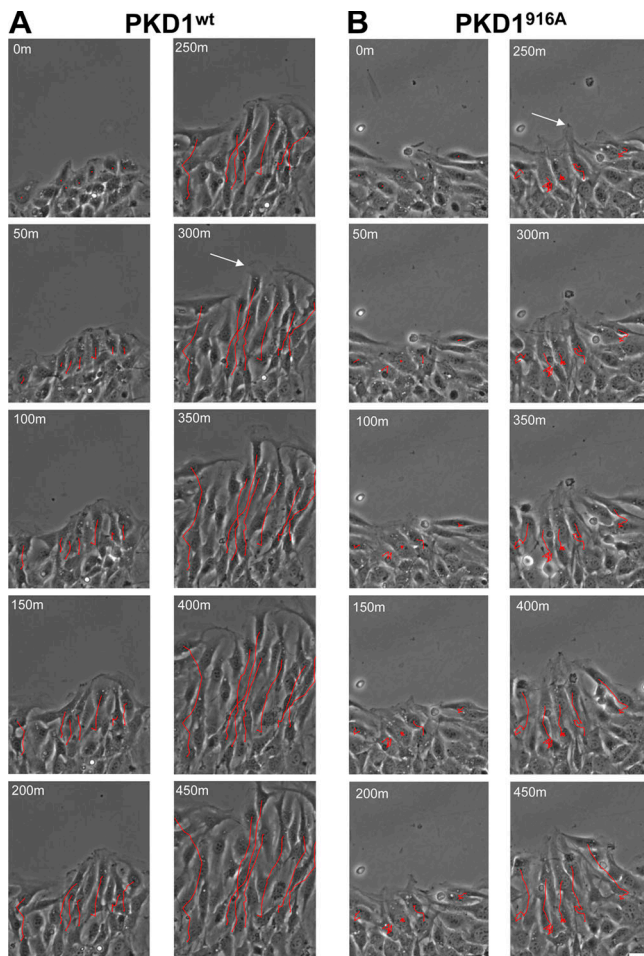


**Figure 3. Effect of PKD1<sup>916A</sup> on the ability of fibroblasts to initiate directional migration after wounding of a monolayer.** NIH3T3 fibroblasts were transfected with either PKD1<sup>wt</sup> (A) or PKD1<sup>916A</sup> (B) using the Nucleofector and grown to confluence over 36 h. Confluent monolayers were wounded with a plastic pipette tip, and the cells were allowed to migrate into the wound. The cells were observed by time-lapse video microscopy, with frames being captured at 20-min intervals. The position of the cell nucleus was followed using cell tracking software, and cumulative track plots of individual cells are displayed in red. The white arrow in (A, 300 min) indicates a cell with a fan-like lamellipodium, the arrow in (B, 250 min) denotes one of the protrusions that form during the migration of PKD1<sup>916A</sup>-expressing cells. Bar, 20  $\mu$ m.

temperature-sensitive (ts) 045 mutant of vesicular stomatitis virus, which is misfolded and retained in the ER at 40°C but moves out of the ER, through the Golgi complex and to the plasma membrane upon temperature shift to 32°C (Presley et al., 1997). ts045 VSVG appeared at the plasma membrane over a time course of  $\sim$ 2 h after shift to 32°C and, consistent with the previously established role of PKD1 in TGN to plasma membrane transport (Liljedahl et al., 2001), this was markedly reduced by expression of a short hairpin RNA (shRNA) targeting PKD1 (Fig. 2 E). However, expression of PKD1<sup>916A</sup> did not suppress delivery of VSVG to the plasma membrane (Fig. 2 E), indicating that although this mutant kinase completely ablated growth factor-driven  $\alpha$ v $\beta$ 3 recycling (Fig. 2, A and B), it did not compromise PKD1's action at the TGN. Collectively, these data highlight the potential effectiveness of PKD1<sup>916A</sup> as a molecular tool, not only to enable comparison of the respective roles played by PKD1

in Golgi transport and integrin recycling but, more particularly, to determine the contribution made by short-loop  $\alpha$ v $\beta$ 3 recycling to cell migration.

### Short-loop $\alpha$ v $\beta$ 3 recycling influences the persistence of cell migration

We (Woods et al., 2004) and others (Prigozhina and Waterman-Storer, 2004) previously determined that suppression of PKD1 leads to reduced cell migration and an impaired ability of migrating fibroblasts to establish their characteristic fan-like morphology. To determine the precise contribution of short-loop  $\alpha$ v $\beta$ 3 recycling to cell migration, we manipulated  $\alpha$ v $\beta$ 3-PKD1 association and Rab4-dependent recycling in fibroblasts, collected time-lapse videos of these cells migrating into a scratch wound, and followed individual cell movement using cell-tracking software. Expression of PKD1<sup>916A</sup> compromised the ability of cells to migrate directionally into the wound (Fig. 3) and, rather than migrating with the fan-like morphology characteristic of fibroblasts (Fig. 3 A, arrow at 300-min time point), PKD1<sup>916A</sup>-expressing cells appeared to migrate by extending thin and often pointed protrusions (Fig. 3 B, arrow at 250-min time point). We therefore proceeded with a more in-depth analysis involving the assembly of overlays of representative trajectories described by cells during the first 5 h of their migration into the wound (Fig. 4 A) and the extraction of parameters such as the persistence and speed of migration from track plots (Fig. 4, B and C), persistence being defined as the ratio of the vectorial distance traveled to the total path length described by the cell. Untransfected fibroblasts and those expressing wild-type PKD1, Rab4, or control shRNA migrated largely perpendicular to the wound edge and maintained a high degree of persistence (Fig. 4 A). However, suppression of short-loop  $\alpha$ v $\beta$ 3 recycling, by PKD1<sup>916A</sup>, RNAi of PKD1, or dominant-negative Rab4, markedly reduced persistent migration such that the cells migrated randomly for up to 5 h after wounding. It is interesting to note that expression of PKD1<sup>916A</sup> or Rab4<sup>121I</sup> (both of which suppress short-loop recycling of  $\alpha$ v $\beta$ 3) reduced persistence without greatly affecting the migration speed, whereas RNAi of PKD1 (which affects both integrin recycling and TGN anterograde transport) reduced both the speed and persistence of migration (Fig. 4, B and C). Moreover, migrational persistence was unaltered by inhibition of long-loop recycling by dominant-negative Rab11, indicating that this key parameter of cell movement relies particularly on the short-loop pathway. To further investigate the requirement for short-loop recycling in migrational persistence, we used a strategy by which endogenous levels of mouse  $\alpha$ v $\beta$ 3 integrin were reduced by expression of a shRNA targeting the mouse sequence of  $\beta$ 3 integrin (Fig. S2, available at <http://www.jcb.org/cgi/content/full/jcb.200609004/DC1>), followed by expression of either the wild-type human  $\alpha$ v $\beta$ 3 heterodimer or  $\beta$ 3 integrins with cytodomain mutations that reduce binding to PKD1. Clearly, suppression of  $\alpha$ v $\beta$ 3 levels by shRNAi profoundly reduced migrational persistence without much affecting the speed of migration (Fig. 4), and persistence was completely restored by expression of human  $\alpha$ v $\beta$ 3 integrin or a  $\beta$ 3 integrin mutant ( $\beta$ 3<sup>G761A</sup>; Woods et al., 2004) with an unaltered ability to recruit PKD1 (Fig. 4). In contrast,  $\beta$ 3 integrin

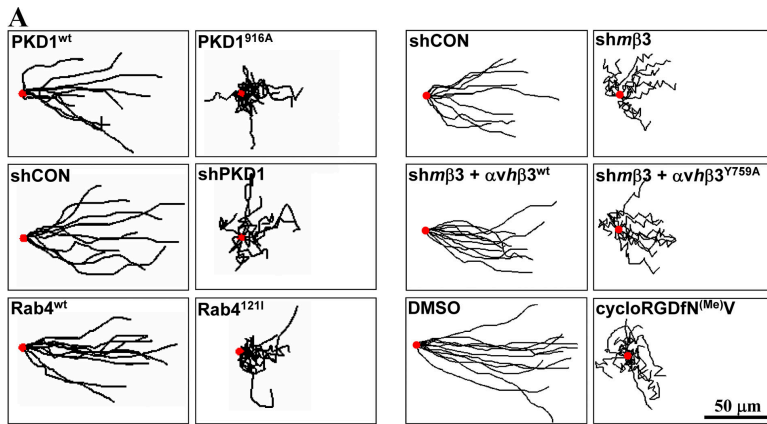
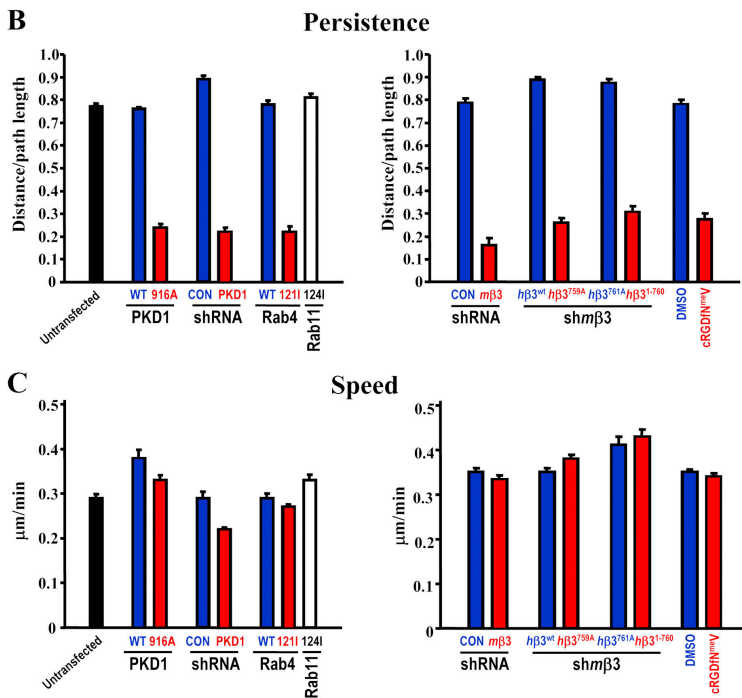


**Figure 4. Blockade of  $\alpha v\beta 3$  integrin short-loop recycling or its ability to engage ECM ligand suppresses the migrational persistence of fibroblasts.** Using the Nucleofector, NIH3T3 fibroblasts were transfected with PKD1<sup>wt</sup>, PKD1<sup>916A</sup>, a control shRNA (shCON), a shRNA-targeting PKD1, Rab4<sup>wt</sup>, or dominant-negative Rab4<sup>121I</sup> or Rab11<sup>124I</sup>. Alternatively, cells were transfected with a shRNA targeting mouse  $\beta 3$  integrin (shm $\beta 3$ ) either alone or in combination with human  $\alpha v$  integrin and the indicated mutants of human  $\beta 3$  integrin ( $\beta 3$ ). Confluent monolayers were wounded with a plastic pipette tip, and the cells were allowed to migrate into the wound in DME supplemented with 10% FCS in the absence or presence of 1  $\mu$ M cyclo-Arg-Gly-Asp-D-Phe-N(Me)-Val (cRGDfN<sup>MeV</sup>) or vehicle control (DMSO). The cells were observed by time-lapse video microscopy, the movement of individual cells followed using cell-tracking software, and this is presented as overlays of representative trajectories described by cells during the first 5 h of their migration into the wound (A). The persistence (B) and speed (C) of migration were extracted from the track plots. Persistence is defined as the ratio of the vectorial distance traveled to the total path length described by the cell. Values are mean  $\pm$  SEM ( $n > 150$  track plots). Bar, 50  $\mu$ m.



mutants ( $\beta 3^{Y759A}$  and  $\beta 3^{1-760}$ ) that cannot bind PKD1 and are consequently unable to enter the short-loop pathway (Woods et al., 2004) do not restore persistent migration in  $\beta 3$  knockdown cells (Fig. 4, A and B). Moreover, a similar reduction in persistence was observed after the addition of a cyclic peptide (cyclo-RGDfN<sup>MeV</sup>) that competitively inhibits binding of ECM ligands to  $\alpha v$  (but not  $\beta 1$ ) integrins (Fig. 4, A and B; Dechantsreiter et al., 1999), indicating that  $\alpha v\beta 3$  needs not only be competent to recycle via the short loop but must also engage ligand to support persistent and directional fibroblast migration.

It is now generally accepted that there is considerable interplay between cytoskeletal events directing cell polarization and the vesicular transport machinery. Indeed, the way that receptors are targeted to the plasma membrane can influence the generation and maintenance of cell polarity and vice versa. We therefore determined whether blockade of short-loop  $\alpha v\beta 3$  recycling altered the ability of cells to polarize their microtubule organizing center (MTOC) in response to wounding. Anterior orientation of the MTOC was detectable shortly after wounding, and this reached a maximum (which was largely maintained)

after 2 h (Fig. 5, A and B). The rate at which MTOC orientation was initiated and the extent to which it was maintained was unaffected by expression of either PKD1<sup>916A</sup> or Rab4<sup>121I</sup> (Fig. 5). This clearly indicated that integrin recycling plays no role in the ability of these cells to sense the wound and polarize their microtubular cytoskeleton accordingly. Moreover, as we continued to track cell movement, it became clear that cells with compromised short-loop recycling, after having migrated randomly for  $\sim 5$  h, began to migrate persistently into the wound (Fig. 6). Collectively, these data indicate that although short-loop  $\alpha v\beta 3$  recycling is not required for wound sensing or the eventual acquisition of a proper migratory phenotype, it is likely to alter signaling events that influence the balance between persistent versus random migration.

#### Short-loop recycling of $\alpha v\beta 3$ opposes $\alpha 5\beta 1$ recycling and resultant signaling to phosphocofilin

Whether a cell chooses persistent over random migration likely depends on the balance between  $\alpha v\beta 3$  and  $\alpha 5\beta 1$  integrin

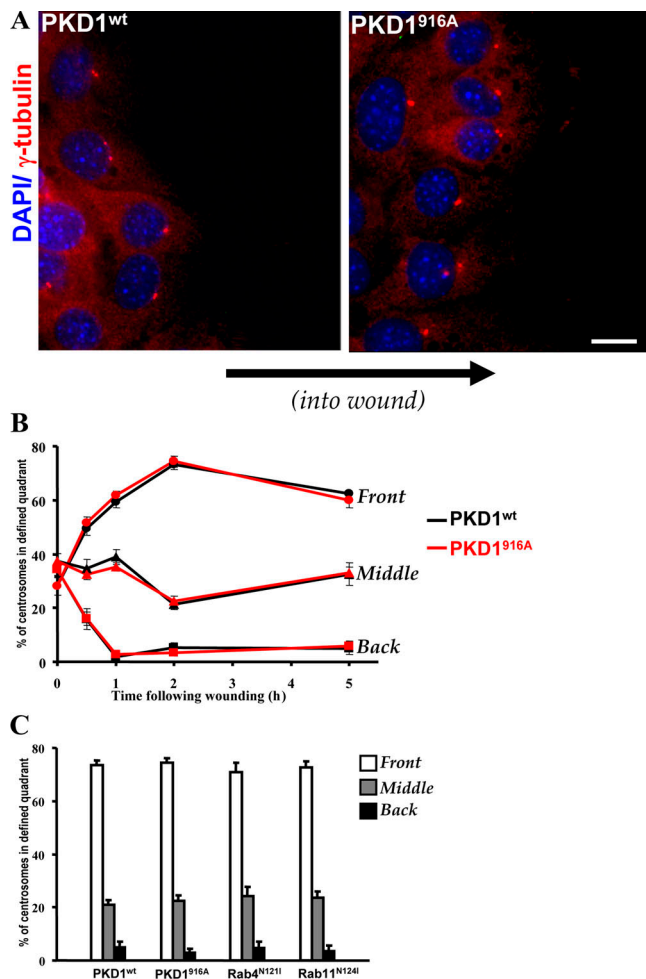


**Figure 5. Short-loop  $\alpha 5 \beta 3$  recycling is not required for orientation of the MTOC.** NIH3T3 fibroblasts were transfected with PKD1<sup>wt</sup>, PKD1<sup>916A</sup>, or dominant-negative Rab4<sup>121I</sup> or Rab11<sup>124I</sup> using the Nucleofector and grown to confluence over 36 h. Confluent monolayers were wounded with a plastic pipette tip, and the cells were allowed to migrate into the wound for 2 h (A and C) or for the times indicated in B. Cells were fixed in ice-cold methanol and the MTOC (centrosomes) visualized by immunofluorescence using an antibody recognizing  $\gamma$ -tubulin (red), and the nucleus was counterstained with DAPI (blue). The position of each centrosome in the first row of cells migrating into the wound was scored according to its position relative to the nucleus. Values are mean  $\pm$  SEM ( $n > 100$  cells). Bar, 10  $\mu$ m.

signaling. It is thought that  $\alpha 5 \beta 3$  promotes persistent and directional migration and that this requires appropriate levels of Rac signaling downstream of this integrin (Danen et al., 2005). Conversely,  $\alpha 5 \beta 1$  tends to promote random migration, and this is a consequence of its ability to activate the Rho–ROCK–cofilin pathway (Danen et al., 2005). Indeed, the increased cellular phospho-Ser<sup>3</sup>-cofilin levels that result from  $\alpha 5 \beta 1$ -driven activation of Rho (and expression of a Ser<sup>3</sup>-phosphomimetic mutant of cofilin) strongly suppress persistence and promote random migration (Danen et al., 2005). As it is possible that the nature of signaling downstream of integrins may be dictated by their trafficking, we investigated whether the influence of the short-loop  $\alpha 5 \beta 3$  recycling pathway on migrational persistence could be indirectly implemented through  $\alpha 5 \beta 1$  recycling and signaling. Indeed, manipulations that compromise the short-loop recycling of  $\alpha 5 \beta 3$  (such as expression of PKD1<sup>916A</sup>, dominant-negative Rab4,

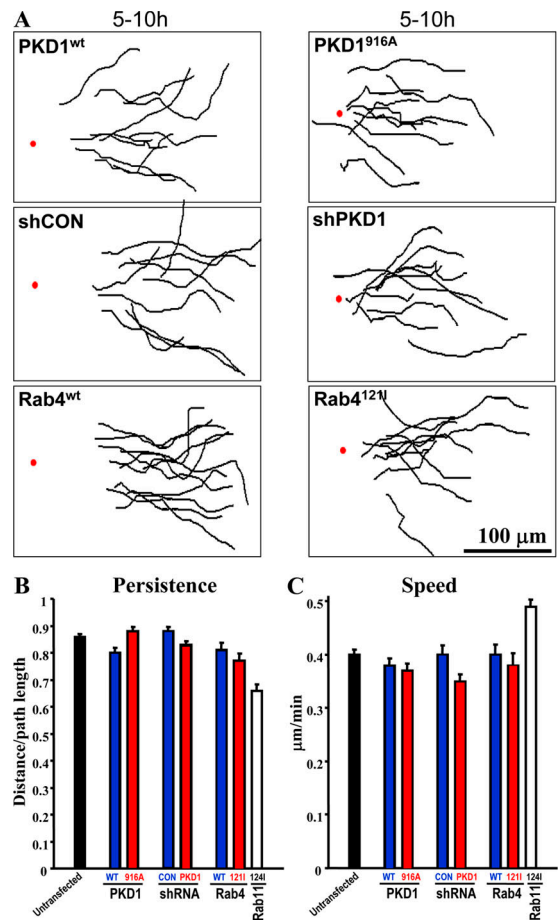


**Figure 6. Cells with compromised short-loop recycling are able to migrate persistently at later times after wounding.** Representative track plots (A) and values of migrational persistence (B) and speed (C) were obtained as for Fig. 4, but with cell movement being followed between 5 and 10 h after wounding. The track plots are from the same cells as those presented in Fig. 4. Values are mean  $\pm$  SEM ( $n > 150$  track plots). Bar, 100  $\mu$ m.

or PKD1 binding-deficient  $\beta 3$  integrin mutants  $\beta 3^{759A}$  and  $\beta 3^{1-760}$ ) acted to increase the rate at which  $\alpha 5 \beta 1$  was returned to the plasma membrane by at least twofold (Fig. 7 A). Conversely, overexpression of wild-type  $\alpha 5 \beta 3$  or a “control”  $\beta 3$  integrin mutant ( $\beta 3^{761A}$ ) that binds to PKD1 profoundly suppressed  $\alpha 5 \beta 1$  recycling (Fig. 7 A). Furthermore, in experiments where cells were either spread onto fibronectin for 30 min or wounded with a pipette tip and then analyzed by Western blotting, phospho-Ser<sup>3</sup>-cofilin levels were markedly promoted by inhibition of  $\alpha 5 \beta 3$  recycling, and the use of an  $\alpha 5 \beta 1$  function-blocking antibody (mAb16) and a ROCK inhibitor (Y27632) indicated that this increase in phosphocofilin was dependent on both  $\alpha 5$  integrin and ROCK (Fig. 7, B and C). Moreover, PKD1<sup>916A</sup>-driven increases in phosphocofilin were only detectable up to 5 h after wounding (i.e., during the period in which cells were migrating randomly); thereafter, levels of this index of ROCK signaling were indistinguishable from that of control cells (Fig. 7 D). Collectively, these observations show a clear reciprocal relationship between short-loop  $\alpha 5 \beta 3$  recycling and the trafficking of  $\alpha 5 \beta 1$  and ability of this integrin to act via ROCK to promote cofilin phosphorylation. In addition, the time course



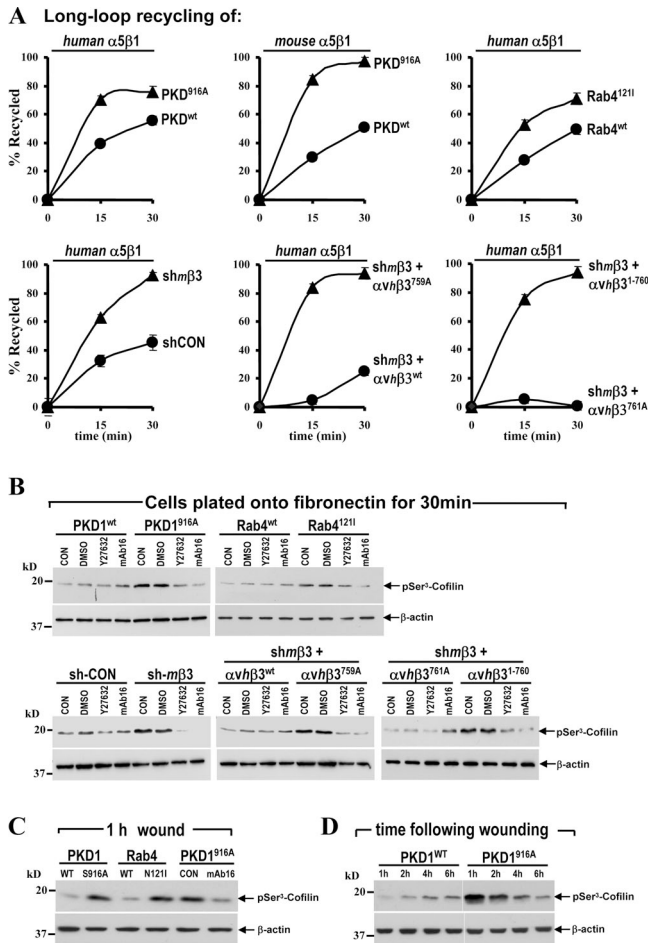


**Figure 7. Inhibition of short-loop recycling of  $\alpha 5 \beta 1$  promotes  $\alpha 5 \beta 1$  recycling and  $\alpha 5 \beta 1$ -dependent ROCK-cofilin signaling.** (A) NIH3T3 fibroblasts were transfected with  $\alpha 5 \beta 1$  integrin (human sequence) together with PKD1<sup>wt</sup>, PKD1<sup>916A</sup>, Rab4<sup>wt</sup>, Rab4<sup>1211</sup>, a nontargeting shRNA (shCON), or a shRNA targeting mouse  $\beta 3$  integrin (sh $\beta 3$ ) either alone or in combination with human  $\alpha v$  integrin and the indicated mutants of human  $\beta 3$  integrin (h $\beta 3$ ). Long-loop recycling of the transfected human  $\alpha 5 \beta 1$  was then determined as described previously (Roberts et al., 2004). To determine recycling of endogenous mouse  $\alpha 5 \beta 1$  (top middle), NIH3T3 fibroblasts were transfected with PKD1<sup>wt</sup> or PKD1<sup>916A</sup> using the Nucleofector. Long-loop recycling of endogenous mouse  $\alpha 5 \beta 1$  was then determined as described by Roberts et al. (2001). Values are mean  $\pm$  SEM ( $n = 10$ ). (B–D) Using the Nucleofector, cells were transfected with PKD1<sup>wt</sup>, PKD1<sup>916A</sup>, Rab4<sup>wt</sup>, Rab4<sup>1211</sup>, a nontargeting shRNA (shCON), or a shRNA targeting mouse  $\beta 3$  integrin (sh $\beta 3$ ) either alone or in combination with human  $\alpha v$  integrin and the indicated mutants of human  $\beta 3$  integrin (h $\beta 3$ ). Cells were grown to confluence over 36 h, trypsinized, incubated in suspension for 45 min, and plated onto plastic surfaces coated with fibronectin (10  $\mu$ g/ml in PBS) for 30 min (B). Where indicated, 2  $\mu$ M Y27632, 2  $\mu$ g/ml mAb16, or vehicle control (DMSO) were included 15 min before and throughout the plating period (B). Alternatively, monolayers were extensively wounded (evenly spaced 500- $\mu$ m wounds; wounded area was  $\sim$ 30% of monolayer area) with a plastic pipette tip, and cells were allowed to migrate into the wound for 1 h (C) or for the times indicated in D. Cells were lysed, and the cellular content of phospho-Ser<sup>3</sup>-cofilin (top) and  $\beta$ -actin (bottom) was determined by Western blotting.

of Rho signaling downstream of  $\alpha 5 \beta 1$  inversely correlates with migrational persistence in a way that accounts for the resumption of this mode of migration at later times after monolayer wounding (compare Fig. 3 B and Fig. 6 with Fig. 7 D).

Given these relationships, we sought to directly determine whether the loss of persistence resulting from inhibition of the

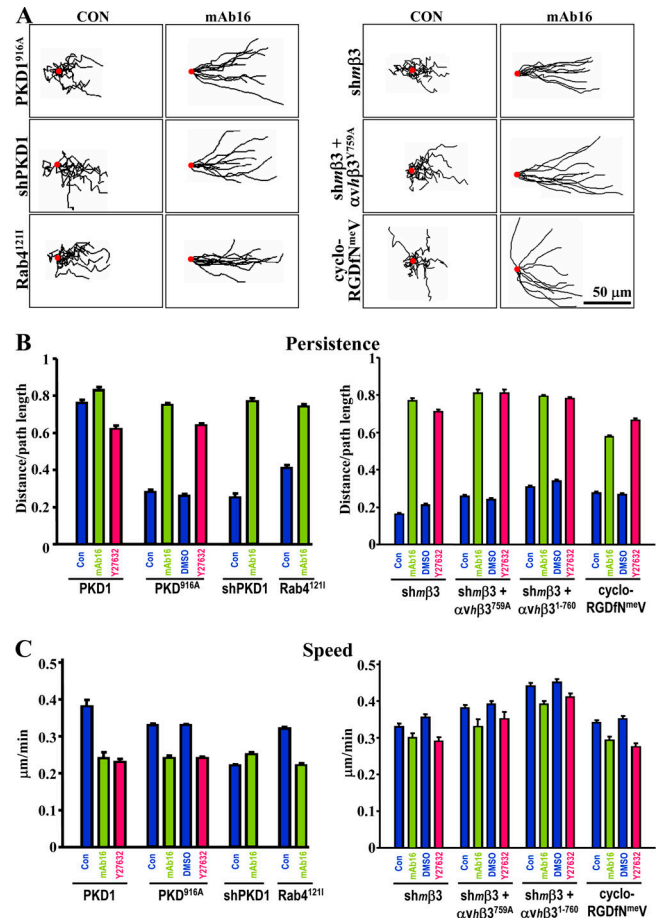


**Figure 8.  $\alpha 5 \beta 1$  function-blocking antibody (mAb16) and ROCK inhibitor (Y27632) restore persistent migration in cells with compromised short-loop recycling.** Using the Nucleofector, NIH3T3 fibroblasts were transfected with PKD1<sup>wt</sup>, PKD1<sup>916A</sup>, a shRNA targeting PKD1 (shPKD1), Rab4<sup>1211</sup>, or a shRNA targeting mouse  $\beta 3$  integrin (sh $\beta 3$ ) either alone or in combination with human  $\alpha v$  integrin and the indicated mutants of human  $\beta 3$  integrin (h $\beta 3$ ). Representative track plots (A) and values for migrational persistence (B) and speed (C) during the first 5 h after monolayer wounding were obtained as for Fig. 4. Where indicated, 2  $\mu$ M Y27632, 2  $\mu$ g/ml mAb16, vehicle control (DMSO), or 1  $\mu$ M cyclo-Arg-Gly-Asp-D-Phe-N(Me)-Val (cRGDfN<sup>m</sup>EV) were added immediately after wounding. Values are mean  $\pm$  SEM ( $n > 75$  track plots). Bar, 50  $\mu$ m.

short-loop pathway was a consequence of increased  $\alpha 5 \beta 1$  signaling. Indeed, addition of mAb16 or Y27632 restored persistent migration in cells expressing PKD1<sup>916A</sup>, shRNAs targeting PKD1, dominant-negative Rab4, or PKD1 binding-deficient  $\beta 3$  integrin mutants (Fig. 8, A and B). Moreover, persistent migration was partially restored by inhibition of  $\alpha 5 \beta 1$  or ROCK signaling in cells treated with cyclo-RGDfNmeV to block the interaction of  $\alpha v \beta 3$  with its ECM ligands (Fig. 8, A and B). These data clearly show that the requirement for  $\alpha v \beta 3$  short-loop recycling (and its ligand engagement) in persistent migration is neither direct nor absolute but is mediated via the ability of this pathway (when active) to antagonize  $\alpha 5 \beta 1$  integrin recycling and subsequent signaling to the ROCK cofilin pathway (Fig. 9 A). Thus, when the  $\alpha v \beta 3$  short loop is blocked, the resulting deregulation of  $\alpha 5 \beta 1$  recycling and signaling promotes random migration in favor of persistence (Fig. 9 B).

## Discussion

PKD1 is thought to promote the fission of vesicles emanating from the TGN and thus enhance the transport of Golgi-derived cargo to the plasma membrane (Liljedahl et al., 2001). However, this has been controversial because of difficulties in demonstrating localization of PKD1 to the TGN (Rey et al., 2001) and the fact that evidence supporting a role for the kinase in Golgi to plasma membrane transport has come primarily from the use of kinase-dead mutants. Despite these caveats, the recent identification of the Golgi-localized phosphatidylinositol 4-kinase III $\beta$  as a physiological PKD substrate (Hausser et al., 2005) and our observation that RNAi of PKD1 suppresses plasma membrane delivery of VSVG protein clearly support a role for this kinase in Golgi to plasma membrane transport. Furthermore, observations of TGN-derived vesicles being transported toward the lamellipodium as fibroblasts migrate (Schmoranzler et al., 2003; Prigozhina and Waterman-Storer, 2004) demand that a contribution of PKD1-regulated Golgi transport to cell migration must be considered. Here, we show that the functional significance of autophosphorylation of PKD1 at Ser<sup>916</sup> is to regulate direct interaction with  $\alpha\beta 3$  and thus influence integrin recycling. However, as phosphorylation at this residue has no detectable effect on the transport of VSVG protein from the TGN to the plasma membrane, we have been able to use PKD1<sup>916A</sup> as a molecular tool to address key questions concerning the relative contributions of PKD1-regulated Golgi transport and integrin recycling to cell migration. First, differential effects of PKD1<sup>916A</sup> on  $\alpha\beta 3$  recycling and VSVG transport indicate that this integrin is unlikely to return to the plasma membrane via the TGN (as is the case for certain recycling proteins). Second, suppression of PKD1 activity by expression of kinase-dead PKD1 or by RNAi influences both speed and directionality, whereas expression of PKD1<sup>916A</sup> selectively targets migrational persistence. This indicates that PKD1 controls  $\alpha\beta 3$  recycling to influence directionality, with PKD1-regulated Golgi traffic acting to additionally enhance the migration speed of fibroblasts.

Although the surface distribution of  $\alpha\beta 3$  in migrating fibroblasts is polarized toward the cell front (Woods et al., 2004), Rab4 is tightly localized to endosomes in the juxtanuclear region that face the direction of travel (unpublished data). Thus, the relevant matrix receptors and the endosomes that traffic them are distributed along the lamellipodial–perinuclear axis of the migrating cell. Moreover, this level of organization depends on flux of  $\alpha\beta 3$  through the short loop, as expression of PKD1<sup>916A</sup> or PKD1 binding–deficient  $\beta 3$  integrins dissipates the polarized distribution of surface  $\alpha\beta 3$  (Woods et al., 2004; unpublished data) and delocalizes Rab4 endosomes from the anterior perinuclear zone (unpublished data). Given these observations, it is tempting to suggest that the short loop directly reinforces persistent migration by transporting  $\alpha\beta 3$  to and from the lamellipodium along the axis of polarity. However, inhibition of  $\alpha 5\beta 1$  signaling in cells with compromised  $\alpha\beta 3$  short-loop recycling enables persistent migration despite a lack of proper polarization of  $\alpha\beta 3$  and Rab4. Therefore, although the short loop may indeed transport  $\alpha\beta 3$  toward the leading

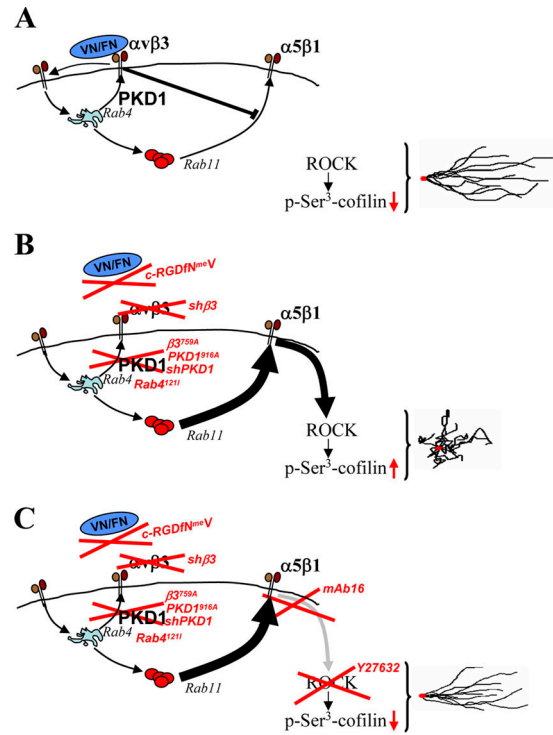


**Figure 9. Schematic summary of the relationship between  $\alpha\beta 3$  and  $\alpha 5\beta 1$  integrin recycling, ROCK signaling, and migrational persistence in fibroblasts.** (A)  $\alpha\beta 3$  integrin is internalized and recycles rapidly via the short-loop pathway under the control of Rab4 and PKD1 to engage ECM ligand (VN/FN). This process exerts a tonic inhibition on the return of internalized  $\alpha 5\beta 1$  integrin from the Rab11 compartment to the plasma membrane. Under these circumstances,  $\alpha 5\beta 1$  has little or no ability to promote cofilin phosphorylation via the ROCK pathway, and cells migrate persistently. (B) After disruption of the short-loop pathway (by RNAi of PKD1, expression PKD1<sup>916A</sup>, dominant-negative Rab4, or  $\beta 3$  mutants that cannot bind PKD1), reduction of  $\alpha\beta 3$  levels by shRNA or pharmacological blockade of its interaction with ECM ligand (c-RGDN<sup>mV</sup>), the rate at which  $\alpha 5\beta 1$  recycles from the Rab11 compartment is increased (bold arrow). Under these circumstances,  $\alpha 5\beta 1$  promotes ROCK-dependent cofilin phosphorylation and migrational persistence is suppressed. (C) When short-loop recycling or  $\alpha\beta 3$  engagement is suppressed, addition of an  $\alpha 5\beta 1$  function-blocking antibody (mAb16) or a ROCK inhibitor (Y27632) reduces phosphocofilin levels, and the cells migrate persistently.

edge, this process is not an absolute requirement for persistent migration when the  $\alpha 5\beta 1$ –ROCK–cofilin pathway is down-regulated. In addition to generating polarized surface distributions and restricting signaling spatially (Jekely et al., 2005), endocytosis/recycling can oppose receptor desensitization (Odley et al., 2004), in part by acting to clear occupied receptors of ligand and returning them to the plasma membrane competent to bind fresh ligand. As our data indicate that  $\alpha\beta 3$  needs to be both rapidly cycling and competent to engage ligand to promote persistent migration, it is probable that short-loop recycling acts to continuously resensitize  $\alpha\beta 3$  to ligand occupation, thus maintaining sufficient  $\alpha\beta 3$  downstream signaling to tonically inhibit  $\alpha 5\beta 1$  recycling.

Epithelial cells expressing  $\alpha\beta 3$  (and not  $\alpha 5\beta 1$ ) migrate persistently, and the appropriate activation of Rac by this integrin is likely to be key to this process (Danen et al., 2005). Conversely, if cells express  $\alpha 5\beta 1$  (and not  $\alpha\beta 3$ ), they migrate randomly because of activation of the ROCK–cofilin pathway



and the antagonistic effect this has on Rac-driven stabilization of the lamellipod (Danen et al., 2005). Therefore, under situations where the expression profile of fibronectin-binding integrins is biased, one is able to predict a cell's migratory behavior. However, in fibroblasts and endothelial cells,  $\alpha 5\beta 1$  and  $\alpha v\beta 3$  expression is closely matched and, because of the relatively small size of the intracellular pool of these integrins ( $\sim 10$  and 20% of the quantity of surface integrin for  $\alpha v\beta 3$  and  $\alpha 5\beta 1$ , respectively) and their capacity to reach the plasma membrane via more than one route, experimental manipulations that target particular integrin recycling pathways (such as those used in the present study) do not greatly alter the amount of  $\alpha v\beta 3$  or  $\alpha 5\beta 1$  that is expressed at the cell surface (Fig. S3, available at <http://www.jcb.org/cgi/content/full/jcb.200609004/DC1>). There is a clear reciprocal relationship between the rates at which  $\alpha v\beta 3$  and  $\alpha 5\beta 1$  recycle; i.e., blockade of  $\alpha v\beta 3$  short-loop recycling doubles the rate at which  $\alpha 5\beta 1$  returns to the plasma membrane via the Rab11 pathway. The mechanistic connection underlying this relationship is not mediated by alterations in PKB/GSK-3 $\beta$  signaling (unpublished data), but the rapidity of  $\alpha 5\beta 1$  recycling is closely correlated with the intensity of cofilin signaling downstream of this integrin. Thus, the way in which an integrin is handled by the recycling pathway may dictate its ability to connect with and activate Rho-signaling pathways. Furthermore, our data suggest that the contribution of recycling to migrational persistence is more easily interpreted in terms of its influence on the signaling capacity of integrins rather than processes such as vectorial transport of matrix receptors to the leading edge and their subsequent incorporation into the adhesive and migratory machine. It is now becoming more apparent that the characteristics of signaling downstream of receptor tyrosine kinases and G protein-coupled receptors depend on how they are trafficked through the endosomal and recycling pathways (Miaczynska et al., 2004). In this regard, it will be interesting to investigate a potential role for the Rab11 pathway in resensitization and prolongation of  $\alpha 5\beta 1$  signaling and whether recycling endosomes constitute a platform for assembly of signalosomes that include guanine nucleotide exchange factors or GTPase-activating proteins for RhoA. In addition to Rho GTPase signaling, ligation of  $\alpha 5\beta 1$  integrin has been linked to activation of Calmodulin-dependent protein kinase II (CamKII) in myeloid cells (Blystone et al., 1999). Furthermore, as ligation of  $\alpha v\beta 3$  strongly suppresses the ability of  $\alpha 5\beta 1$  to communicate with CamKII, the possibility that this and other examples of integrin "cross-talk" involve alterations in the endo-exocytic behavior of  $\alpha 5\beta 1$  should be considered.

Using a strategy to selectively target the Rab4-dependent short-loop recycling of  $\alpha v\beta 3$  integrin, we demonstrate a clear connection between this pathway and a persistent mode of fibroblast migration. Short-loop recycling exerts its influence by counteracting the trafficking and signaling of another integrin, the  $\alpha 5\beta 1$  heterodimer, and there is no obligatory requirement for short-loop  $\alpha v\beta 3$  recycling when  $\alpha 5\beta 1$  signaling is compromised. These data show that the short loop does not form part of the machinery integral to persistent cell migration, but acts to dictate the nature of integrin downstream signaling, which in turn influences the cell's decision to migrate with persistence or to

move randomly on 2D matrices. The ability of  $\beta 1$  integrins to signal to RhoA determines the mode of tumor cell invasiveness (Vial et al., 2003), and a key challenge for the future will be to determine the influence that recycling pathways have on integrin signaling and the choice between elongated and amoeboid migration of tumor cells through 3D matrices.

## Materials and methods

### Plasmids

$\alpha v$ ,  $\beta 3$ ,  $\alpha 5$ , and  $\beta 1$  integrins and Rab4, Rab4<sup>1211</sup>, and Rab11<sup>1241</sup> were in pcDNA3 are as described by Roberts et al. (2001) and Woods et al. (2004). The mouse sequences for PKD1 and PKD1<sup>916A</sup> were tagged with a hexa-Histidine at the 5' end (N terminus), cloned into pcDNA3, and verified by sequencing. The shRNA mU6pro vector targeting PKD1 and the validation of its efficacy is described by Woods et al. (2004), and the shRNA sequences targeting mouse  $\beta 3$  integrin (5'-CAGCTCATTGTTGATGCTT-3' and 5'-GTCAGCCTTTACCAGAATT-3') were cloned into the mU6pro vector as described by Yu et al. (2002). tsO45-VSVG is as described previously (Presley et al., 1997) and was a gift from J. Lippincott-Schwartz (National Institutes of Health, Bethesda, MD). All plasmids were purified by CsCl banding before transfection into NIH3T3 fibroblasts by Fugene 6 or Amaxa Nucleofection. PCR-amplified DNA fragment corresponding to the indicated regions of the human sequence of  $\beta 3$  integrin were subcloned into the pGEX-4T-1 vector. GST fusion proteins were expressed in *Escherichia coli* strain BL-21 and purified as described previously (Woods et al., 2002).

### Expression and purification of His-PKD1

Cos-1 cells transfected with His-PKD1 or His-PKD1<sup>916A</sup> were treated with 1  $\mu$ M PMA for 15 min to activate the kinase and then lysed in 200 mM NaCl, 75 mM Tris, 15 mM NaF, 1.5 mM Na<sub>3</sub>VO<sub>4</sub>, 7.5 mM EDTA, 7.5 mM EGTA, 1.5% Triton X-100, 0.75% Igepal CA-630, 50  $\mu$ g/ml leupeptin, 50  $\mu$ g/ml aprotinin, and aminoethyl benzene sulfonyl fluoride (AEBSF) and scraped from the dish with a rubber policeman. Lysates were passed three times through a 27-gauge needle and clarified by centrifugation at 10,000 g for 10 min. The clarified lysates were loaded into a 1-ml His-TRAP affinity column (GE Healthcare), and the kinase was eluted with a linear gradient of imidazole. 1-ml fractions were collected, and the peak of purified His-PKD1 was identified by SDS-PAGE followed by staining with colloidal Coomassie. The kinase was dialysed overnight into kinase buffer (25 mM Hepes, pH 7.4, containing 25 mM MgCl<sub>2</sub>, 0.5 mM Na<sub>3</sub>VO<sub>4</sub>, 0.5 mM EDTA, and 0.5 mM DTT), glycerol was added to 50% (vol/vol), and the kinase was stored at  $-20^{\circ}\text{C}$ . Kinase assays to assess the catalytic activity of PKD1 were performed in kinase buffer in the presence of 100  $\mu$ M ATP, 4.4  $\mu$ Ci  $\gamma$ -[<sup>32</sup>P]ATP, and 3  $\mu$ g c-Jun 1–89 GST fusion protein (a gift from M. Dickens, University of Leicester, Leicester, UK) per reaction. Reaction products were resolved in 12% SDS-polyacrylamide gels, which were dried and exposed to x-ray film to visualize bands.

### Microtitre ELISA

GST-integrin cytodomain fusion proteins were bound at saturating concentrations to wells of microtitre plates (Immuno. 2; Dynatech Laboratories) in 0.05 M Na<sub>2</sub>CO<sub>3</sub>, pH 9.6, at 4 $^{\circ}$ C, and the wells were blocked with PBS containing 0.1% (vol/vol) Tween-20 (PBS-T). Various amounts of purified His-PKD1 or His-PKD1<sup>916A</sup> were added to the wells in PBS-T and incubated for 1 h at 15 $^{\circ}$ C. After three washes with PBS-T, PKD1 was detected by serial incubations with polyclonal rabbit anti-PKC $\mu$  (sc-639; Santa Cruz Biotechnology, Inc.) and horseradish peroxidase-conjugated anti-rabbit IgG, followed by chromogenic reaction with ortho-phenylenediamine as described previously (Roberts et al., 2001).

### Immunoprecipitations

Cells were grown to 90% confluence, serum-starved for 30 min, and treated with a combination of 10 ng/ml PDGF-BB and 0.6 mM primaquine for 12 min. After this, cells were washed twice in ice-cold PBS, lysed in 200 mM NaCl, 75 mM Tris, 15 mM NaF, 1.5 mM Na<sub>3</sub>VO<sub>4</sub>, 7.5 mM EDTA, 7.5 mM EGTA, 1.0% octyl  $\beta$ -thioglucopyranoside, 50  $\mu$ g/ml leupeptin, 50  $\mu$ g/ml aprotinin, and AEBSF and subjected to immunoprecipitation using magnetic beads coupled to a mouse anti-human  $\beta 3$  integrin monoclonal antibody (clone VI-PL2; BD Biosciences) as described previously (Woods et al., 2004). Unbound proteins were removed by extensive washing in octyl  $\beta$ -thioglucopyranoside-containing buffer and specifically associated proteins resolved by SDS-PAGE (8% gels under reducing conditions for detection of

PKD1; 6% gels under nonreducing conditions for  $\beta 3$  integrin) and analyzed by Western blotting as described previously (Woods et al., 2004).

#### Cell culture and transfection

NIH3T3 mouse fibroblasts and Cos-1 cells were grown in DME with 10% (vol/vol) fetal calf serum and 100 U/ml penicillin, 100  $\mu$ g/ml streptomycin, and 0.25  $\mu$ g/ml amphotericin B at 37°C with 10% CO<sub>2</sub>. For integrin recycling assays, immunoprecipitations, and preparation of purified PKD1, cells were grown to 50% confluence, fed with fresh DME containing 10% (vol/vol) fetal calf serum, and transfected using Fugene 6 (Roche Diagnostics) according to the manufacturer's instructions. The ratio of Fugene 6 to DNA was maintained at 3  $\mu$ l Fugene/1  $\mu$ g DNA. For cell migration studies and measurement of phosphocofilin signaling, transfections were performed using the Nucleofector system (Amaxa). In brief, cells were grown to 80% confluence, removed by trypsinization, washed in PBS, and resuspended in Amaxa solution R with 5  $\mu$ g DNA. After electroporation (in the Nucleofector; program T-20), the cells were replated in 6-well dishes.

#### Receptor recycling and Golgi transport assays

Integrin recycling assays were performed as described previously (Roberts et al., 2001). <sup>125</sup>I-transferrin recycling assays were performed essentially as described previously (van Dam and Stoorvogel, 2002) with some modifications. In brief, serum-starved cells were incubated with <sup>125</sup>I-labeled transferrin (0.1  $\mu$ Ci/well; NEX212 [NEN Life Science Products]) for 1 h at 4°C in PBS with 1% (wt/vol) BSA. The tracer was allowed to internalize for 15 min at 22°C (to label early endosomes) or 30 min at 37°C (to label the recycling compartment). Tracer remaining at the cell surface was removed by incubation with acid-PBS (corrected to pH 4.0 by the addition of HCl) at 4°C for 6 min, and the tracer was allowed to recycle at 37°C in serum-free DME supplemented with 1% BSA and 50  $\mu$ M desferoxamine (D9533; Sigma-Aldrich). The quantity of <sup>125</sup>I recycled into the medium is expressed as a percentage of the number of counts incorporated during the internalization period.

For measurement of Golgi transport, NIH3T3 fibroblasts were transfected with tsO45 VSVG and placed at 40°C for 24 h. Cells were then incubated at 32°C for the indicated times and placed on ice. Surface proteins were labeled by incubation with 0.2 mg/ml NHS-Biotin (EZ-Link Sulfo-NHS-Biotin [21217]; Pierce & Warriner) in PBS for 30 min at 4°C, and biotinylated VSVG was detected by capture ELISA using microtitre wells coated with a polyclonal antibody recognizing VSVG (ab3861; Abcam).

#### Time-lapse microscopy and track-plot analysis

Confluent monolayers were wounded with a plastic pipette tip and placed on the stage of an inverted microscope (Axiovert S100; Carl Zeiss Microimaging, Inc.) in an atmosphere of 5% CO<sub>2</sub> at 37°C. Cells were observed using a 20 $\times$  phase-contrast objective, and images were collected every 20 min using a digital camera (C4742-95; Hamamatsu). Videos were generated and cell tracks analyzed using Andor Bioimaging software. The selective  $\alpha$ v integrin antagonist cyclic peptide, cyclo-Arg-Gly-Asp-D-Phe-N(Me)-Val (cRGDFN<sup>me</sup>V), was as described by Dechantsreiter et al. (1999) and was added to the monolayers shortly after wounding at a concentration of 1  $\mu$ M.

#### Analysis of MTOC polarization

Wounded monolayers were maintained at 37°C for various times and fixed in ice-cold methanol. Fixed cells were incubated with an anti- $\gamma$ -tubulin monoclonal antibody (clone GTU-88; Sigma-Aldrich), followed by a Texas red-conjugated secondary antibody and counterstaining with DAPI to visualize nuclei. The percentage of cells with the MTOC positioned in quadrants facing the wound (front) or at the cell rear (back) or neither (middle) with respect to the position of the nucleus was determined by visual examination of images captured on an epifluorescence microscope (AxioPhot; Carl Zeiss Microimaging, Inc.).

#### Measurement of phosphocofilin signaling

Cells transfected using the Nucleofector were trypsinized, incubated in suspension for 45 min, and plated onto plastic surfaces coated with 10  $\mu$ g/ml fibronectin. Where indicated, 2  $\mu$ M Y27632 (Calbiochem) or 2  $\mu$ g/ml mAb16 (a gift from K. Yamada, National Institutes of Health, Bethesda, MD) were included 15 min before and throughout the plating period. Alternatively, monolayers were extensively wounded (evenly spaced 500- $\mu$ m wounds; wounded area was ~30% of monolayer area) with a plastic pipette tip, and cells were allowed to migrate into the wound for various times. Cells were lysed and subjected to Western blotting followed by detection with an antibody recognizing phospho-Ser<sup>3</sup>-cofilin (3311; Cell Signaling Technologies).

#### Online supplemental material

Fig. S1 shows that overexpression of recombinant His-PKD1s inhibits activation of endogenous PKD1. Fig. S2 shows use of shRNAi to suppress cellular levels of mouse  $\alpha$ v $\beta$ 3 integrin. Fig. S3 shows the influence of mutant Rab4 and PKD1 on the surface expression of  $\alpha$ v $\beta$ 3 and  $\alpha$ 5 $\beta$ 1 integrins. Fig. S4 shows coimmunoprecipitation of endogenous PKD1 with endogenous mouse  $\alpha$ v $\beta$ 3 integrin. Online supplemental material is available at <http://www.jcb.org/cgi/content/full/jcb.200609004/DC1>.

J.C. Norman and P.T. Caswell were supported by Cancer Research UK at the Beatson Institute for Cancer Research, and D.P. White was supported by grants from the Wellcome Trust and Cancer Research UK.

We would like to thank Ken Yamada for the generous gift of mAb16.

Submitted: 1 September 2006

Accepted: 4 April 2007

## References

- Arias-Salgado, E.G., S. Lizano, S. Sarkar, J.S. Brugge, M.H. Ginsberg, and S.J. Shattil. 2003. Src kinase activation by direct interaction with the integrin beta cytoplasmic domain. *Proc. Natl. Acad. Sci. USA*. 100:13298–13302.
- Arthur, W.T., N.K. Noren, and K. Burridge. 2002. Regulation of Rho family GTPases by cell-cell and cell-matrix adhesion. *Biol. Res*. 35:239–246.
- Blystone, S.D., S.E. Slater, M.P. Williams, M.T. Crow, and E.J. Brown. 1999. A molecular mechanism of integrin crosstalk:  $\alpha$ v $\beta$ 3 suppression of calcium/calmodulin-dependent protein kinase II regulates  $\alpha$ 5 $\beta$ 1 function. *J. Cell Biol.* 145:889–897.
- Bretscher, M.S. 1996. Moving membrane up to the front of migrating cells. *Cell*. 85:465–467.
- Caswell, P.T., and J.C. Norman. 2006. Integrin trafficking and the control of cell migration. *Traffic*. 7:14–21.
- Cox, E.A., S.K. Sastry, and A. Huttenlocher. 2001. Integrin-mediated adhesion regulates cell polarity and membrane protrusion through the Rho family of GTPases. *Mol. Biol. Cell*. 12:265–277.
- Danen, E.H., J. van Rheenen, W. Franken, S. Huveneers, P. Sonneveld, K. Jalink, and A. Sonnenberg. 2005. Integrins control motile strategy through a Rho-cofilin pathway. *J. Cell Biol.* 169:515–526.
- Dechantsreiter, M.A., E. Planker, B. Matha, E. Lohof, G. Holzemann, A. Jonczyk, S.L. Goodman, and H. Kessler. 1999. N-Methylated cyclic RGD peptides as highly active and selective  $\alpha$ (V) $\beta$ (3) integrin antagonists. *J. Med. Chem.* 42:3033–3040.
- Fan, G.H., L.A. Lapierre, J.R. Goldenring, J. Sai, and A. Richmond. 2004. Rab11-family interacting protein 2 and myosin Vb are required for CXCR2 recycling and receptor-mediated chemotaxis. *Mol. Biol. Cell*. 15:2456–2469.
- Hausser, A., P. Storz, S. Martens, G. Link, A. Toker, and K. Pfizenmaier. 2005. Protein kinase D regulates vesicular transport by phosphorylating and activating phosphatidylinositol-4 kinase IIIbeta at the Golgi complex. *Nat. Cell Biol.* 7:880–886.
- Hurd, C., R.T. Waldron, and E. Rozengurt. 2002. Protein kinase D complexes with C-Jun N-terminal kinase via activation loop phosphorylation and phosphorylates the C-Jun N-terminus. *Oncogene*. 21:2154–2160.
- Hynes, R.O. 2002. Integrins: bidirectional, allosteric signaling machines. *Cell*. 110:673–687.
- Jekely, G., H.H. Sung, C.M. Luque, and P. Rorth. 2005. Regulators of endocytosis maintain localized receptor tyrosine kinase signaling in guided migration. *Dev. Cell*. 9:197–207.
- Jones, M.C., P.T. Caswell, and J.C. Norman. 2006. Endocytic recycling pathways: emerging regulators of cell migration. *Curr. Opin. Cell Biol.* 18:549–557.
- Liljedahl, M., Y. Maeda, A. Colanzi, I. Ayala, J. Van Lint, and V. Malhotra. 2001. Protein kinase D regulates the fission of cell surface destined transport carriers from the trans-Golgi network. *Cell*. 104:409–420.
- Matthews, S.A., E. Rozengurt, and D. Cantrell. 1999. Characterization of serine 916 as an in vivo autophosphorylation site for protein kinase D/Protein kinase Cmu. *J. Biol. Chem.* 274:26543–26549.
- Miaczynska, M., L. Pelkmans, and M. Zerial. 2004. Not just a sink: endosomes in control of signal transduction. *Curr. Opin. Cell Biol.* 16:400–406.
- Odley, A., H.S. Hahn, R.A. Lynch, Y. Marreze, H. Osinska, J. Robbins, and G.W. Dorn II. 2004. Regulation of cardiac contractility by Rab4-modulated beta2-adrenergic receptor recycling. *Proc. Natl. Acad. Sci. USA*. 101:7082–7087.
- Pankov, R., Y. Endo, S. Even-Ram, M. Araki, K. Clark, E. Cukierman, K. Matsumoto, and K.M. Yamada. 2005. A Rac switch regulates random versus directionally persistent cell migration. *J. Cell Biol.* 170:793–802.

- Presley, J.F., N.B. Cole, T.A. Schroer, K. Hirschberg, K.J. Zaal, and J. Lippincott-Schwartz. 1997. ER-to-Golgi transport visualized in living cells. *Nature*. 389:81–85.
- Prigozhina, N.L., and C.M. Waterman-Storer. 2004. Protein kinase D-mediated anterograde membrane trafficking is required for fibroblast motility. *Curr. Biol.* 14:88–98.
- Rey, O., S.H. Young, D. Cantrell, and E. Rozengurt. 2001. Rapid protein kinase D translocation in response to G protein-coupled receptor activation. Dependence on protein kinase C. *J. Biol. Chem.* 276:32616–32626.
- Roberts, M., S. Barry, A. Woods, P. van der Sluijs, and J. Norman. 2001. PDGF-regulated rab4-dependent recycling of alphavbeta3 integrin from early endosomes is necessary for cell adhesion and spreading. *Curr. Biol.* 11:1392–1402.
- Roberts, M.S., A.J. Woods, T.C. Dale, P. Van Der Sluijs, and J.C. Norman. 2004. Protein kinase B/Akt acts via glycogen synthase kinase 3 to regulate recycling of alpha v beta 3 and alpha 5 beta 1 integrins. *Mol. Cell. Biol.* 24:1505–1515.
- Sanchez-Ruiloba, L., N. Cabrera-Poch, M. Rodriguez-Martinez, C. Lopez-Menendez, R.M. Jean-Mairet, A.M. Higuero, and T. Iglesias. 2006. Protein kinase D intracellular localization and activity control kinase D-interacting substrate of 220-kDa traffic through a postsynaptic density-95/discs large/zonula occludens-1-binding motif. *J. Biol. Chem.* 281:18888–18900.
- Schmoranzler, J., G. Kreitzer, and S.M. Simon. 2003. Migrating fibroblasts perform polarized, microtubule-dependent exocytosis towards the leading edge. *J. Cell Sci.* 116:4513–4519.
- van Dam, E.M., and W. Stoorvogel. 2002. Dynamin-dependent transferrin receptor recycling by endosome-derived clathrin-coated vesicles. *Mol. Biol. Cell.* 13:169–182.
- Vertommen, D., M. Rider, Y. Ni, E. Waelkens, W. Merlevede, J.R. Vandenhede, and J. Van Lint. 2000. Regulation of protein kinase D by multisite phosphorylation. Identification of phosphorylation sites by mass spectrometry and characterization by site-directed mutagenesis. *J. Biol. Chem.* 275:19567–19576.
- Vial, E., E. Sahai, and C.J. Marshall. 2003. ERK-MAPK signaling coordinately regulates activity of Rac1 and RhoA for tumor cell motility. *Cancer Cell.* 4:67–79.
- Woods, A.J., M.S. Roberts, J. Choudhary, S.T. Barry, Y. Mazaki, H. Sabe, S.J. Morley, D.R. Critchley, and J.C. Norman. 2002. Paxillin associates with poly(A)-binding protein 1 at the dense endoplasmic reticulum and the leading edge of migrating cells. *J. Biol. Chem.* 277:6428–6437.
- Woods, A.J., D.P. White, P.T. Caswell, and J.C. Norman. 2004. PKD1/PKCmu promotes alphavbeta3 integrin recycling and delivery to nascent focal adhesions. *EMBO J.* 23:2531–2543.
- Yu, J.Y., S.L. DeRuiter, and D.L. Turner. 2002. RNA interference by expression of short-interfering RNAs and hairpin RNAs in mammalian cells. *Proc. Natl. Acad. Sci. USA.* 99:6047–6052.